2012

The local metallicity of gadolinium doped compound semiconductors

J. A. Colon Santana

Pan Liu

Xianjie Wang

J. Tang

S. R. McHale

See next page for additional authors

Authors
J. A. Colon Santana, Pan Liu, Xianjie Wang, J. Tang, S. R. McHale, D. Wooten, J. W. McClory, J. C. Petrosky, J. Wu, R. Palai, Ya B. Losovjy, and P. A. Dowben

J. Phys.: Condens. Matter **24** (2012) 445801 (6pp) doi:10.1088/0953-8984/24/44/445801

The local metallicity of gadolinium doped compound semiconductors

J A Colón Santana[1], Pan Liu[2], Xianjie Wang[2], J Tang[2], S R McHale[3], D Wooten[3], J W McClory[3], J C Petrosky[3], J Wu[4], R Palai[4], Ya B Losovjy[5] and P A Dowben[5]

[1] Department of Electrical Engineering, W Scott Engineering Center, University of Nebraska, North 16th Street, Lincoln, NE 68588-0656, USA
[2] Department of Physics and Astronomy, University of Wyoming, Laramie, WY 82071, USA
[3] Air Force Institute of Technology, 2950 Hobson Way, Wright Patterson Air Force Base, OH 45433, USA
[4] Department of Physics and Institute for Functional Nanomaterials, University of Puerto Rico, Rio Piedras, Natural Sciences Building, Phase II, San Juan, PR 00931, USA
[5] Department of Physics and Astronomy and Nebraska Center for Materials and Nanoscience, University of Nebraska-Lincoln, Theodore Jorgensen Hall, 855 North 16th Street, Lincoln, NE 68588-0299, USA

E-mail: pdowben@unl.edu

Received 16 August 2012
Published 9 October 2012
Online at stacks.iop.org/JPhysCM/24/445801

Abstract
The local metallicities of $Hf_{0.97}Gd_{0.03}O_2$, $Ga_{0.97}Gd_{0.03}N$, $Eu_{0.97}Gd_{0.04}O$ and EuO films were studied through a comparison of the findings from constant initial state spectroscopy using synchrotron light. Resonant enhancements, corresponding to the 4d → 4f transitions of Eu and Gd, were observed in some of the valence band photoemission features. The resonant photoemission intensity enhancements for the Gd 4f photoemission features are far stronger for the more insulating host systems than for the metallic system $Eu_{0.96}Gd_{0.04}O$. The evidence seems to suggest a correlation between the effective screening in the films and the resonant photoemission process.

(Some figures may appear in colour only in the online journal)

1. Introduction

Gadolinium is usually treated as having a stable 3+ valence when inserted into host semiconductors, and yet the effect of increasing gadolinium concentration is very different in different semiconductors. Gadolinium is a p-type dopant in HfO_2 [1–3] and an n-type dopant in EuO [4] and 4% replacement (or less) of Eu in EuO with gadolinium will drive EuO across the nonmetal to metal transition [4–6]. Caution must be applied though when dealing with the metallicity of overlayers, thin films or surfaces [7]. The use of resonant photoemission or constant initial state spectroscopy has been a useful tool to probe metallicity in thin films [7–23] and although the metallic behavior of $Eu_{0.96}Gd_{0.04}O$ has been established [4], resonant photoemission provides an independent means for testing the metallicity $Eu_{1-x}Gd_xO$.

A major attribute of resonant photoemission is that it allows one to distinguish which valence bands of the semiconductor host have strong rare earth 4f and/or simply rare earth weight [23–30]. The 4d–4f photoemission resonances for various rare earth doped GaN thin films (RE = Gd, Er, Yb) have now been reported [24–29], and like studies of Gd doped HfO_2 [30], permit a fairly definitive placement of the rare earth 4f states in the valence band.

In processes such as photoemission, excitons may be formed and are expected to be affected by the screening at some extent; this is especially true for a resonant photoemission process [7–14]. Once the insulating system makes the transition to the metallic phase, free carriers are expected to reduce the Coulomb field between the electron and the hole and shorten the lifetime of the core exciton [31, 32]. Under this assumption, resonant photoemission intensity scales proportionally with the square root of the effective mass and inversely proportional with the screening parameter l_s as:

$$\left(\frac{1}{l_s}\right)^2 = \left(\frac{I}{I_0}\right)^2 = \frac{m^*}{m_e} \quad (1)$$

where the screening parameter affects the potential roughly as:

$$U(r) = -\frac{e^2}{r}\exp(-l_s r). \quad (2)$$

This suggests that an increase in screening, due to an increase of carrier concentration, can lead to a diminution of the resonant photoemission peak intensity, and this is in fact generally supported by experiment [7–24, 33]. In fact this can be a local probe of charge localization [17, 33]. Here we broaden the concept of screening and metallicity, as probed by resonant photoemission, by comparing the resonant photoemission enhancement of the valence band features of semiconducting $Gd_{0.03}Ga_{0.97}N$ and $Gd_{0.03}Hf_{0.97}O_2$ to the more metallic $Eu_{0.96}Gd_{0.04}O$.

2. Experimental details

The Gd doped (3 at.%) HfO_2 films were deposited on p-type Si(100) using pulsed laser deposition (PLD) and grown at a rate of about 0.15 Å s^{-1}, as described elsewhere [1–3, 30]. The deposition was performed at a substrate temperature of 500 °C. The chamber was pumped to a base pressure of 3×10^{-7} Torr and the deposition was carried out in a mixture of H_2 and Ar (8% H_2) to introduce the necessary oxygen vacancies.

The EuO and $Eu_{0.96}Gd_{0.04}O$ films were also deposited on Si(100) using pulsed laser deposition, as previously described [4, 34]. Before the deposition the silicon wafers were annealed at a temperature of 750 °C inside the vacuum chamber at a pressure of 10^{-5} Torr under pure-H_2 gas to enhance removal of the native SiO_2 surface layer. The targets used in the PLD process were either Eu (99.9%) metal or a mixture of Eu (99.9%) or Gd (99.9%) metals, and the purity of H_2 gas used during the deposition was 99.995%.

The $Gd_xGa_{1-x}N$ thin films were fabricated on Si(111) substrates by RF plasma (EPI 620) assisted molecular beam epitaxy (MBE). The growth parameters for the deposition of Gd doped (*in situ*) GaN thin films were base pressure of approximately 10^{-11} Torr, nitrogen flux of 0.75–1.0 SCCM, RF power of 500 W, substrate temperature of 850–900 °C, Ga cell temperature of 850 °C, and Gd cell temperatures of 1050–1100 °C, as previously described [28, 29, 35].

The photoemission experiments were conducted on the 3 m TGM beamline [36] at the Center for Advanced Microstructures and Devices at Louisiana State University [37–39]. The beamline is equipped with a photoemission endstation with a 50 mm hemispherical electron energy analyzer, with a resolution of about 70 meV, as described elsewhere [36, 40]. Photoemission spectra were taken with a 45° incidence angle and the photoelectrons collected along the sample normal. All spectra presented are normalized to the photon flux, and the secondary electron background has been subtracted. The position of the Fermi level was established using a clean Ta foil as reference. All binding energies reported here are with respect to this common Fermi level in terms of E–E_F, so that occupied state binding energies are negative. Energy distribution curves (EDCs) were obtained by fixing the photon energy $h\nu$ and sweeping electron kinetic energy E_K, thus measuring binding energies. Constant initial state spectra were obtained by simultaneously sweeping $h\nu$ and E_K, so as to hold fixed the binding energy.

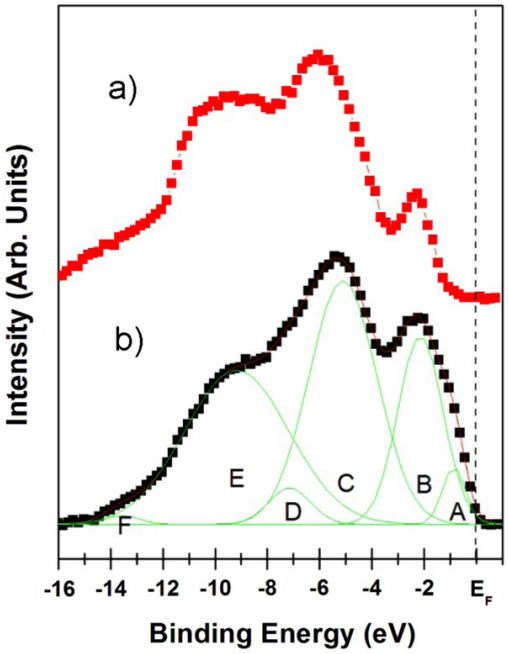

Figure 1. Valence band spectra obtained from the photoemission density of state for (a) EuO and (b) $Eu_{0.96}Gd_{0.04}O$ films grown on p-type Si(100). The composition of the spectra was determined by the Gaussian distributions and the photoemission features were classified as arising from largely the (A) Eu $4d_{5/2}$ and electron pockets of the conduction band minimum, (B) Eu $4d_{3/2}$, (C) O 2s, (D) O 2s and Eu 4f final state (satellite) contributions and (E) Gd 4f and Eu 4f final state (satellite) contributions. Photoelectrons were collected along the surface normal. Measurements for both films were taken using synchrotron light with photon energy of 60 eV and incidence angle of 45°. Binding energy is denoted in terms of E–E_F.

3. Resonant photoemission in EuO films

Core to this study are the valence band intensities of $Eu_{0.96}Gd_{0.04}O$ through the 4d to 4f super Coster–Kronig photoemission resonance. The valence band photoemission features for both EuO and $Eu_{0.96}Gd_{0.04}O$ contain a number of shake up features [4], so that off resonance, at photon energies well away from a Eu or Gd 4d core level binding energy, the spectra for both the doped and undoped samples are similar, as seen in figure 1. Contributions corresponding to the Eu 4f final states in EuO are observed at a binding energy of −2.3 eV followed by a strong weighted O 2p features −4 to −6 eV, consistent with GW calculations [41]. The broad unresolved photoemission feature located at −7 to −11 eV stem from a variety of configurations of the final state excited state and Eu 4f satellite features [4, 42].

The inclusion of small amounts of gadolinium in the EuO lattice has little effect on the valence band structure, but changes near the Fermi level are also observed as suggested by the increase in the photoemission density of states. Increases

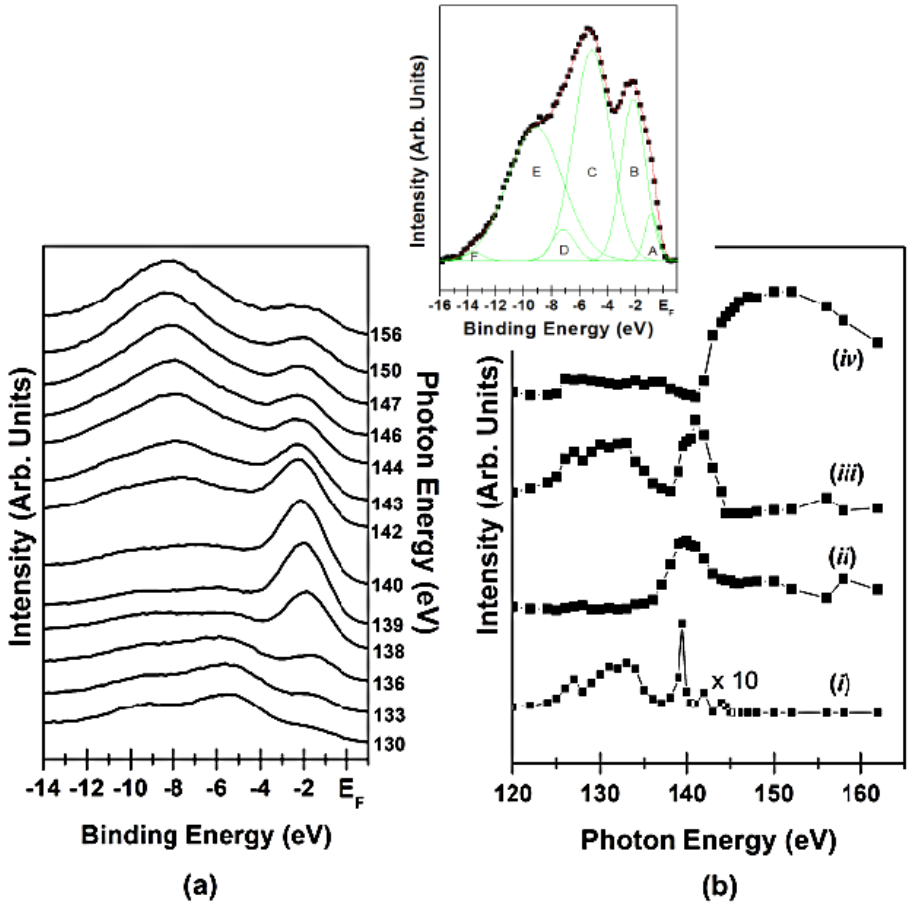

Figure 2. (a) The photoemission spectra for photon energies through the Gd and Eu 4d to 4f super Coster–Kronig photoemission resonance for $Eu_{0.96}Gd_{0.04}O$ films. (b) The resonant photoemission intensities, as a function of photon energy i.e. constant initial state spectra, for the valence feature at (i) 0.5 eV, (ii) 2.3 eV, (iii) 6.1 eV and (iv) 9.2 eV below the Fermi level. Light was incident at 45°. Photoelectrons were collected along the surface normal. Binding energy is denoted in terms of E–E_F.

in the photoemission density of states near the Fermi level in the doped films have been observed and are attributable to an increase in metallicity as demonstrated by mapping the electronic band structure near the Fermi level along both the crystallographic direction of the $Eu_{0.96}Gd_{0.04}O$ films and along the $\overline{\Gamma X}$ symmetry line in reciprocal space [4].

The contributions to the valence band region from the Gd 4f orbital in the valence band spectra are more transparent for photon energies that correspond to the 4d to 4f super Coster–Kronig photoemission resonance, as indicated in figure 2(a). The strongest enhancements in the valence band region of the photoemission spectra occur in the photon energy range of 130–160 eV, but we find that the different photoemission features resonate at different photon energies (figure 2(b)), reflecting differences in the origin of their spectral weight. Because of the multi-configurational final states originating from EuO itself, a unique assignment of one feature to Gd alone is difficult, but we expect that the Gd 4f spectral weight should be largely located in the region of −9 eV binding energy [24–30, 33], as discussed below.

The enhancements originating from the Eu $4f^6$ final state configuration are observed in the features near the Fermi level ((i) in figure 2(b)) at about −6 eV binding energy ((iii) in figure 2(b)). Excitations involving a final state $4f^6$ are also evident as shown by (ii). In this case, the resonant photoemission process is described by a resonant process that includes direct photoionization:

$$4d^{10}\,4f^7 + h\nu \rightarrow 4d^{10}\,4f^6 + e^- \tag{3}$$

that is supplemented by a super Coster–Kronig transition of the form:

$$4d^{10}\,4f^7 + h\nu \rightarrow 4d^9\,4f^8 \rightarrow 4d^{10}\,4f^6 + e^- \tag{4}$$

which results in the same final state. The resonant enhancement, seen in figure 2, of the feature at about −6 eV binding energy (figure 2(b), iii) that occurs at photon energies of 130 and 140 eV suggests strong hybridization of the europium atoms with oxygen. At photon energies near 130 eV, one expects contributions from the Eu $4d_{5/2}$ to dominate while oxygen photoemission resonances do not occur near these photon energies. This enhancement provides a clear indication of the strong hybridization between the Eu 5d6s and oxygen 2p contributions.

Resonant enhancements of the feature at a binding energy of about −9.2 eV (iv, in figure 2) occur at photon energies close to the core threshold binding energy of the Gd $4d_{3/2}$ shallow core (about 147 eV), also as a result of a $4f^6$ final state,

again dominated by excitations (3) and (4). This too leads to the classic Fano resonances seen in (iv) in figure 2(b). This feature in the region of −9 eV binding energy is not purely Gd in weight though, as seen in figure 1 and discussed above. Unlike the other semiconductors studied here, contributions from Eu $4f^5$ final states are expected at similar binding energies (approximately −9 eV) via different excitation and decay channels [42]. In fact excitations of the form

$$4d^{10}\,4f^7(5d6s6p)^2 + h\nu \rightarrow 4d^{10}\,4f^5 4d\,(5d6s6p)^3 + e^- \quad (5a)$$

$$4d^{10}\,4f^7(5d6s6p)^2 + h\nu \rightarrow 4d^9\,4f^7(5d6s6p)^3 \rightarrow 4d^{10}\,4f^5(5d6s6p)^3 + e^- \quad (5b)$$

$$4d^{10}\,4f^7(5d6s6p)^2 + h\nu \rightarrow 4d^9\,4f^8(5d6s6p)^2 \rightarrow 4d^{10}\,4f^5(5d6s6p)^3 + e^- \quad (5c)$$

are expected to contribute to the Fano-resonance seen (figure 2) for the $Eu_{0.96}Gd_{0.04}O$ photoemission feature at −9.2 eV (iv), i.e. the multi-configurational final state. The contributions from the various multi-configurational final states are what provide the large width, in photon energy, of the resonance line shape (figure 2(b) (iv)).

4. Comparing the Gd 4d to 4f photoemission resonance for Gd in various host semiconductors

Although complications arise from the Eu 4d → 4f contributions to the Gd 4d → 4f super Coster–Kronig transition in the resonant photoemission processes for $Eu_{0.96}Gd_{0.04}O$, in fact the Gd 4d → 4f transition resonance for $Eu_{0.96}Gd_{0.04}O$ is similar to the resonances in the photoemission valence band with photon energy, seen in $Gd_{0.03}Ga_{0.97}N$ and $Gd_{0.03}Hf_{0.97}O_2$. Figure 3 shows the valence band photoemission spectra for $Eu_{0.96}Gd_{0.04}O$, $Gd_{0.03}Ga_{0.97}N$, $Gd_{0.03}Hf_{0.97}O_2$ at the Gd 4d → 4f photoemission resonance ('on' with $h\nu = 147$ eV) and away from the photoemission resonance ('off' with $h\nu =$ 140, 139.7 and 132 eV for $Eu_{0.96}Gd_{0.04}O$, $Gd_{0.03}Ga_{0.97}N$, $Gd_{0.03}Hf_{0.97}O_2$ respectively). As expected [24–30], there is a noticeable enhancement of the photoemission in intensity at the Gd 4d → 4f photoemission resonance (i.e. 'on' resonance at $h\nu = 147$ eV), in the region of the Gd 4f binding energy at 8–20 eV below the Fermi level in the valence band photoemission spectra for $Eu_{0.96}Gd_{0.04}O$, $Gd_{0.03}Ga_{0.97}N$, $Gd_{0.03}Hf_{0.97}O_2$ (figure 3).

In the case of $Gd_{0.04}Eu_{0.96}O$, the Gd 4d → 4f excitation results in the super Coster–Kronig transition and resonant photoemission (equations (3) and (4)), and yet the enhancement ('on' versus 'off') is less pronounced than is observed for $Gd_{0.03}Ga_{0.97}N$ and $Gd_{0.03}Hf_{0.97}O_2$, as seen visually in figure 4 and summarized in table 1. This decrease in the resonant photoemission enhancement is seen to occur even though both Eu (equation (5)) and Gd (equation (4)) both contribute $Gd_{0.04}Eu_{0.96}O$, 4d → 4f excitation resonant photoemission signal in the region of −9 eV binding energy. Thus without a doubt, $Gd_{0.04}Eu_{0.96}O$ is more metallic and better screened (more itinerant electrons) than either $Gd_{0.03}Ga_{0.97}N$ or $Gd_{0.03}Hf_{0.97}O_2$.

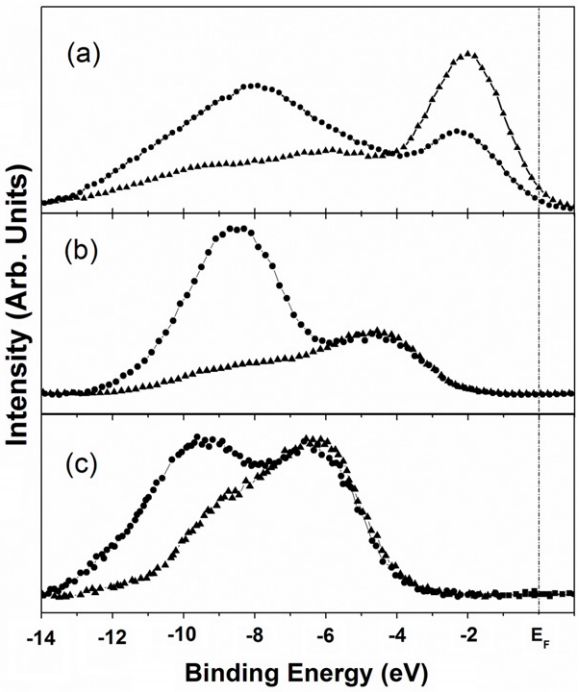

Figure 3. Valence band photoemission spectra 'on' (photon energy of 147 eV) and 'off' (photon energy of 'off' with $h\nu = 140$ eV, 139.7 eV and 132 eV for $Eu_{0.96}Gd_{0.04}O$, $Gd_{0.03}Ga_{0.97}N$, $Gd_{0.03}Hf_{0.97}O_2$ respectively) the Gd 4d to 4f resonant photoemission feature obtained for (a) $Eu_{0.96}Gd_{0.04}O$, (b) $Gd_{0.03}Ga_{0.97}N$ and (c) $Gd_{0.03}Hf_{0.97}O_2$. All photoelectrons were collected along the normal to the film surface. Binding energy is denoted in terms of E–E_F.

Table 1. Summary of the photon energy for resonant photoemission intensity maximum, the width of the Gd 4d to 4f photoemission resonance, in photon energy and the intensity ratio of 'on' resonance at a photon energy given to the 'off' resonant intensity.

Film	Peak position (eV)	Width (eV)	On–off ratio
$Gd_{0.04}Eu_{0.96}O$	150.3	17.25	1.83
$Gd_{0.03}Hf_{0.97}O_2$	149.0	8.96	11.22
$Gd_{0.03}Ga_{0.97}N$	147.9	7.11	9.82

5. Across the nonmetal to metal transition in $Gd_{0.04}Eu_{0.96}O$

Not only is the on–off ratio for the 4d → 4f photoemission resonance much smaller for $Gd_{0.04}Eu_{0.96}O$ than for $Gd_{0.03}Ga_{0.97}N$ and $Gd_{0.03}Hf_{0.97}O_2$, as seen visually in figure 3 but we can also compare the EuO and $Gd_{0.04}Eu_{0.96}O$ 4d → 4f excitation resonant photoemission signal in the region of −2 eV binding energy, as seen in figure 5. This resonant enhancement is almost entirely attributable to just the Eu 4d to 4f excitation and the valence band spectral weight is largely due to the Eu 4f [4, 42]. As with the comparison of the Gd 4d → 4f photoemission resonance for $Gd_{0.04}Eu_{0.96}O$ versus $Gd_{0.03}Ga_{0.97}$ N and $Gd_{0.03}Hf_{0.97}O_2$, where $Gd_{0.04}Eu_{0.96}O$ differs significantly and has a far reduced photoemission resonance, $Gd_{0.04}Eu_{0.96}O$ also has a much reduced Eu 4d → 4f photoemission resonance

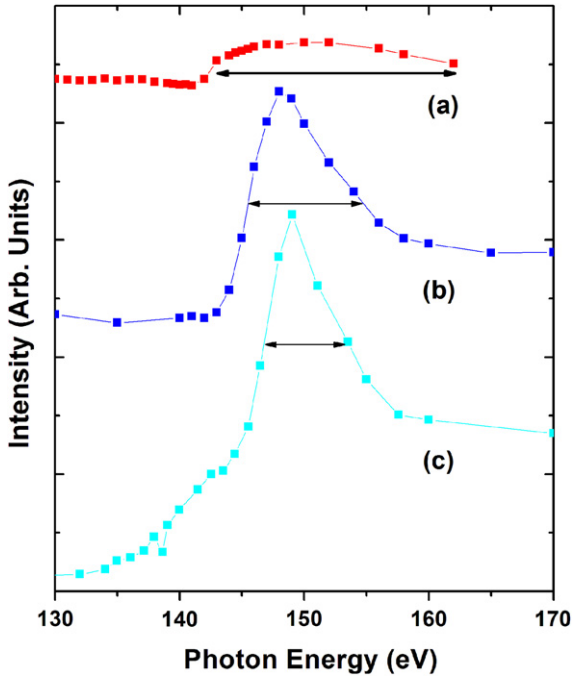

Figure 4. Constant initial state valence intensity as a function of photon energy in the region of Gd 4f contributions to the valence band (at roughly −9 eV binding energy, E–E_F) in Gd doped (a) EuO (4%), (b) GaN (3%), (c) HfO_2 (3%) host systems.

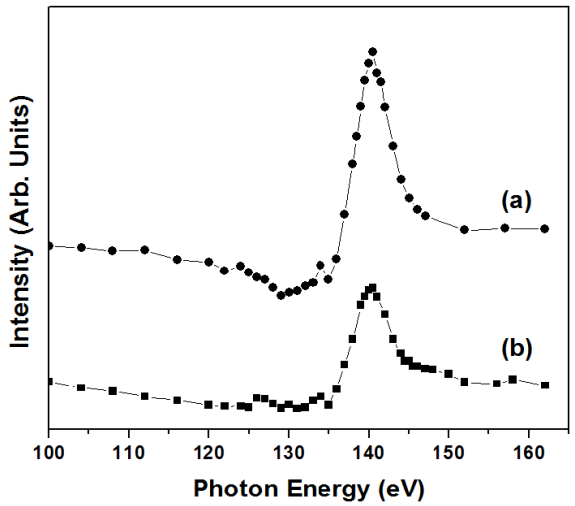

Figure 5. Resonant photoemission intensity as a function of photon energy for the Eu 4f weighted features in the valence band at about −2 eV binding energy (E–E_F) in (a) EuO and (b) $Eu_{0.96}Gd_{0.04}O$ films. The decrease in intensity suggests a major change in metallicity with the inclusion of 4% per cent Gd.

compared to EuO. This effect is consistent with our view of a metal to nonmetal transition with increasing Gd concentration in EuO. Thus while it has been suggested [6] that not all Gd dopant atoms contribute to populating the conduction band electron pocket [4, 5], once the system goes metallic, all Gd and Eu 4f contributions to the valence band appear well screened in the resonant photoemission process.

6. Conclusion

The Eu and Gd 4d → 4f excitation resonant photoemission signal was exploited to probe the metallicity of different Gd doped host systems. Evidence of the metallic behavior of $Eu_{0.96}Gd_{0.04}O$ was confirmed by a significant decrease in the resonant photoemission signal compared to the more insulating system EuO, $Gd_{0.03}Ga_{0.97}N$ and $Gd_{0.03}Hf_{0.97}O_2$. The results reveal a significant effect of the unoccupied band structure and metallicity of Gd doped EuO, $Eu_{0.96}Gd_{0.04}O$, on the 4d–4f resonant photoemission processes that involve both Eu and Gd.

Acknowledgments

This work was supported by the Defense Threat Reduction Agency (DTRA) through Grant No. HDTRA1-07-1-0008 and BRBAA08-I-2-0128, the Institute for Functional Nanomaterials, NASA-IDEA-PR, DOE DE-EE0003174 and the National Science Foundation (Grants No. DMR-0852862, No. CBET-0754821, and the Nebraska Materials Science and Engineering Center (DMR-0820521)). The views expressed in this paper are those of the authors and do not reflect the official policy or position of the Air Force, Department of Defense, or the US Government.

References

[1] Losovyj Y B, Ketsman I, Sokolov A, Belashchenko K D, Dowben P A, Tang J and Wang Z 2007 *Appl. Phys. Lett.* **91** 132908
[2] Ketsman I, Losovyj Y B, Sokolov A, Tang J, Wang Z, Natta M, Brand J I and Dowben P A 2008 *Appl. Surf. Sci.* **254** 4308–12
[3] Schultz D *et al* 2010 *J. Phys. D: Appl. Phys.* **43** 075502
[4] Colón Santana J A, An J M, Wu N, Belashchenko K D, Wang X, Liu P, Tang J, Losovyj Y B, Yakovkin I N and Dowben P A 2012 *Phys. Rev.* B **85** 014406
[5] Shai D E, Melville A J, Harter J W, Monkman E J, Shen D W, Schmehl A, Schlom D G and Shen K M 2012 *Phys. Rev. Lett.* **108** 267003
[6] Mairoser T *et al* 2010 *Phys. Rev. Lett.* **105** 257206
[7] Dowben P A 2000 *Surf. Sci. Rep.* **40** 151–247
[8] Zhang J, Li D and Dowben P A 1993 *Phys. Lett.* A **173** 183–9
[9] Dowben P A, LaGraffe D, Li D, Vidali G, Zhang L, Dottl L and Onellion M 1991 *Phys. Rev.* B **43** 10677–9689
[10] Zhang J, Li D and Dowben P A 1994 *J. Phys.: Condens. Matter* **6** 33–54
[11] Zhang J, McIlroy D N and Dowben P A 1994 *Phys. Rev.* B **49** 13780–6
[12] Zhang J, McIlroy D N and Dowben P A 1995 *Europhys. Lett.* **29** 469–74
[13] Zhang J, McIlroy D N and Dowben P A 1995 *Phys. Rev.* B **52** 11380–6
[14] McIlroy D N, Zhang J, Liou S-H and Dowben P A 1995 *Phys. Lett.* A **207** 367–73
[15] Zhang J, McIlroy D N, Dowben P A, Liou S-H, Sabiryanov S F and Jaswal S S 1996 *Solid State Commun.* **97** 39–44
[16] McIlroy D N, Waldfried C, Zhang J, Choi J-W, Foong F, Liou S-H and Dowben P A 1996 *Phys. Rev.* B **54** 17438
[17] Chung B W, Schwartz A J, Ebbinghaus B B, Fluss M J, Haslam J J, Blobaum K J M and Tobin J G 2006 *J. Phys. Soc. Japan* **75** 054710

[18] Park K T, Cao J, Gao Y and Ruckman M W 1995 *J. Vac. Sci. Technol.* A **13** 200
[19] Wall A, Franciosi A, Gao Y, Weaver J H, Tsai M-H, Dow J D and Kasowski R V 1989 *J. Vac. Sci. Technol.* A **7** 656
[20] Janowitz C, Manzke R, Skibowski M, Takeda Y, Miyamoto Y and Cho C 1992 *Surf. Sci.* **275** L669
[21] Lapeyre G J and Anderson J 1975 *Phys. Rev. Lett.* **35** 117
[22] Lapeyre G J, Baer A D, Hermonson J, Anderson J, Knapp J A and Gobby P L 1974 *Solid State Commun.* **15** 1601
[23] Lapeyre G J, Anderson J, Gobby P L and Knapp J A 1977 *Phys. Rev. Lett.* **33** 1290
[24] Shi J, Chandrashekhar M V S, Reiherzer J, Schaff W, Lu J, Disalvo F and Spencer M G 2008 *Phys. Status Solidi* c **5** 1495
[25] Thomas T, Guo X M, Chandrashekhar M V S, Poitras C B, Shaff W, Dreibelbis M, Reiherzer J, Li K W, Disalvo F J, Lipson M and Spencer M G 2009 *J. Cryst. Growth* **311** 4402–7
[26] Steckl A J, Park J H and Zavada J M 2007 *Mater. Today* **10** 20–7
[27] Dieke G H and Crosswhite H M 1963 *Appl. Opt.* **2** 675–86
[28] McHale S R, McClory J W, Petrosky J C, Wu J, Palai R, Losovyj Y B and Dowben P A 2011 *Eur. Phys. J. Appl. Phys.* **56** 11301
[29] Wang L, Mei W N, McHale S R, McClory J W, Petrosky J C, Wu J, Palai R, Losovyj Y B and Dowben P A 2012 *Semicond. Sci. Technol.* at press
[30] Ketsman I, Losovyj Y B, Sokolov A, Tang J, Wang Z, Belashchenko K D and Dowben P A 2007 *Appl. Phys.* A **89** 489–92
[31] Turkevich L A and Cohen M H 1984 *Phys. Rev. Lett.* **53** 2323
[32] Turkevich L A and Cohen M H 1984 *J. Non-Cryst. Solids* **62** 13
[33] Wu N, LaGraffe D, Yakovkin I N and Dowben P A 2011 *Phys. Status Solidi* b **248** 1253–7
[34] Wang X, Liu P, Fox K A, Tang J, Colón Santana J A, Belashchenko K D, Dowben P A and Sui Y 2010 *IEEE Trans. Magn.* **46** 1879–82
[35] McHale S R, McClory J W, Petrosky J C, Wu J, Rivera A, Palai R, Losovyj Y B and Dowben P A 2011 *Eur. Phys. J. Appl. Phys.* **55** 31301
[36] Losovyj Y, Ketsman I, Morikawa E, Wang Z, Tang J and Dowben P A 2007 *Nucl. Instrum. Methods Phys. Res.* A **582** 264
[37] Hormes J, Scott J D and Suller V P 2006 *Synchrotron Radiat. News* **19** 27
[38] Roy A, Morikawa E, Bellamy H, Kumar C, Goettert J, Suller V, Morris K, Ederer D and Scott J 2007 *Nucl. Instrum. Methods Phys. Res.* A **582** 22–5
[39] Morikawa E, Scott J D, Goettert J, Aigeldinger G, Kumar C S S R, Craft B C, Sprunger P T, Tittsworth R C and Hormes F J 2002 *Rev. Sci. Instrum.* **73** 1680–3
[40] Dowben P A, LaGraffe D and Onellion M 1989 *J. Phys.: Condens. Matter* **1** 6571
[41] An J M, Barabash S V, Ozolins V, van Schilfgaarde M and Belashchenko K D 2011 *Phys. Rev.* B **83** 064105
[42] Schneider W D, Laubschat C, Kalkowski D, Haase J and Puschmann A 1983 *Phys. Rev.* B **28** 2017